MULTIPULSE MULTICARRIER COMMUNICATIONS OVER TIME-VARYING FADING CHANNELS: PERFORMANCE ANALYSIS AND SYSTEM OPTIMIZATION

Manfred M. Hartmann, Gerald Matz, and Dieter Schafhuber

Institut für Nachrichtentechnik und Hochfrequenztechnik, Vienna University of Technology
Gusshausstrasse 25/389, A-1040 Vienna, Austria (Europe)
Tel.: +43 1 58801 38975; Fax: +43 1 58801 38999; Email: manfred.hartmann@nt.tuwien.ac.at

ABSTRACT

We present an interference and noise analysis for *multipulse multicarrier (MPMC)* transmission over time-varying fading channels. Based on this analysis, we propose algorithms and guidelines for system optimization (transmit and receive pulse shapes, time-frequency lattice parameters, and power allocation). Numerical simulations illustrate the optimization gain and the superiority of MPMC systems over traditional (single-pulse) multicarrier systems for highly dispersive channels.

1. INTRODUCTION

Multipulse multicarrier (MPMC) modulation is a recently introduced wireless communication scheme that extends *multicarrier (MC) modulation* by using multiple transmit and receive pulses [1]. In [1], algorithms and examples for the design of MPMC transmit and receive pulses have been presented. The resulting pulses showed excellent time-frequency (TF) concentration which suggests increased interference robustness when transmitting over time-varying frequency-selective channels. MPMC modulation also establishes a unifying framework for existing MC schemes like simple single-pulse MC systems (cyclic-prefix OFDM, pulse-shaping OFDM) [2, 3], multicarrier DS-CDMA [4], OFDM with offset-QAM [5], and MC systems with hexagonal or other non-rectangular TF lattices [6]). The novel contributions of this paper are:

- a detailed noise and interference analysis for MPMC systems transmitting over time-varying fading channels,
- the definition of meaningful performance measures for MPMC systems,
- algorithms and guidelines for the optimization of the transmit and receive pulse shapes, the power allocation, and the lattice parameters of MPMC systems,
- simulation results verifying the optimization gains and the advantage of MPMC systems over single-pulse MC systems.

After discussing the MPMC system model in Section 2, we present an interference analysis in Section 3. This involves a simplified vector channel model and different performance measures that are the basis for our system optimization in Section 4. Section 5 shows simulation results and Section 6 provides conclusions.

2. MPMC SYSTEMS

An MPMC modulator uses R linearly independent transmit pulses $g^{(r)}(t)$, $r = 1,\ldots,R$, to transmit R symbols $a^{(r)}[l,k]$ at symbol time l and subcarrier k. With K subcarriers the transmit signal is [1]

$$s(t) = \sum_{l=-\infty}^{\infty} \sum_{k=0}^{K-1} \mathbf{a}^T[l,k]\, \mathbf{g}_{l,k}(t). \tag{1}$$

Here, $\mathbf{a}[l,k] = \big[a^{(1)}[l,k] \ldots a^{(R)}[l,k]\big]^T$, and $\mathbf{g}_{l,k}(t) = \mathbf{g}(t-lT)\, e^{j2\pi kFt}$ with $\mathbf{g}(t) = \big[g^{(1)}(t) \ldots g^{(R)}(t)\big]^T$. The symbol duration T and the subcarrier spacing F are the MPMC TF lattice parameters.

The signal $s(t)$ is transmitted over a time-varying Rayleigh fading channel $\mathbb{H}$ with impulse response $h(t,\tau)$. The channel satisfies the assumption of *wide-sense stationary uncorrelated scattering (WSSUS)* [7, 8]. The receive signal is given by[1]

$$r(t) = (\mathbb{H}s)(t) + n(t) = \int_\tau h(t,\tau)\, s(t-\tau)\, d\tau + n(t), \tag{2}$$

where $n(t)$ is additive white Gaussian noise (AWGN) of variance σ_n^2. The WSSUS channel $\mathbb{H}$ will be characterized by its *scattering function* (delay-Doppler spectrum) $C_{\mathbb{H}}(\tau,\nu)$ [7, 8] (τ and ν denote time delay and Doppler frequency, respectively). Practical WSSUS channels are *underspread* [8], i.e., the channel spread factor $4\tau_{\max}\nu_{\max}$ is much less than one ($\tau_{\max}$ and $\nu_{\max}$ are the channel's maximum delay and Doppler frequency, respectively).

At the receiver, the MPMC demodulator employs R receive pulses $\gamma^{(r)}(t), r = 1,\ldots,R$, to calculate the receive sequences $x^{(r)}[l,k]$ from $r(t)$ in (2) according to

$$\mathbf{x}[l,k] = \int_t r(t)\, \boldsymbol{\gamma}^*_{l,k}(t)\, dt. \tag{3}$$

Here, $\mathbf{x}[l,k] = \big[x^{(1)}[l,k] \ldots x^{(R)}[l,k]\big]^T$ and $\boldsymbol{\gamma}_{l,k}(t) = \boldsymbol{\gamma}(t-lT)\, e^{j2\pi kFt}$ with $\boldsymbol{\gamma}(t) = \big[\gamma^{(1)}(t) \ldots \gamma^{(R)}(t)\big]^T$.

It can be shown that for ideal channel ($r(t) = s(t)$), perfect symbol recovery ($\mathbf{x}[l,k] = \mathbf{a}[l,k]$) in an MPMC system is obtained if and only if $\mathbf{g}(t)$ and $\boldsymbol{\gamma}(t)$ are *biorthogonal*, i.e.,

$$\int_t \mathbf{g}(t)\, \boldsymbol{\gamma}^H_{l,k}(t)\, dt \;=\; \delta[l]\, \delta[k]\, \mathbf{I}. \tag{4}$$

If in addition $\mathbf{g}(t) = \boldsymbol{\gamma}(t)$, we call the MPMC system orthogonal. (Bi)orthogonal MPMC systems require that $\{\mathbf{g}_{l,k}(t)\}$, $\{\boldsymbol{\gamma}_{l,k}(t)\}$ are *multipulse Gabor Riesz bases* (cf. [1]); this in turn presupposes $TF/R \geq 1$ (consistent with the single-pulse case). Efficient algorithms that calculate a *canonical biorthogonal* pulse $\boldsymbol{\gamma}(t)$ and an orthogonalized pulse $\mathbf{g}^{\perp}(t)$ from a prescribed pulse $\mathbf{g}(t)$ are described in [1]. These algorithms are based on a Zak transform description of MPMC systems. Zak transform formulations also exist for the results and algorithms of the present paper but are not discussed due to lack of space.

Funding by FWF Grant P15156.

[1] Integrals are from $-\infty$ to ∞.

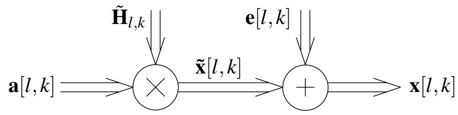

Figure 1: *Equivalent vector channel for MPMC systems.*

3. INTERFERENCE ANALYSIS

Equivalent Vector Channel. For the subsequent interference analysis, we assume the number of subcarriers K to be infinite. The results obtained are upper bounds for the case of finite K which are tight for the subcarriers close to the center frequency if K is sufficiently large. By combining (1), (2), and (3), the input-output relation for the overall MPMC system is obtained as

$$\mathbf{x}[l,k] = \sum_{l'=-\infty}^{\infty} \sum_{k'=-\infty}^{\infty} \mathbf{H}_{l,k;l',k'}\, \mathbf{a}[l',k'] + \mathbf{z}[l,k], \tag{5}$$

with the $R \times R$ channel matrices

$$\mathbf{H}_{l,k;l',k'} = \int_t \boldsymbol{\gamma}_{l,k}^*(t)\, \big(\mathbb{H}\mathbf{g}_{l',k'}^T\big)(t)\, dt,$$

and the noise vector $\mathbf{z}[l,k] = \int_t \boldsymbol{\gamma}_{l,k}^*(t)\, n(t)\, dt$. The terms in (5) with $(l',k') \neq (l,k)$ correspond to *intersymbol interference* (ISI) and *intercarrier interference* (ICI), and the off-diagonal elements in $\mathbf{H}_{l,k;l,k}$ correspond to *interpulse interference* (IPI). For our analysis we define an equivalent vector channel (see Fig. 1)

$$\mathbf{x}[l,k] = \tilde{\mathbf{x}}[l,k] + \mathbf{e}[l,k], \tag{6}$$

where $\mathbf{e}[l,k]$ subsumes all undesired interference and noise, and the desired receive vector is ($\odot$ denotes the Hadamard product)

$$\tilde{\mathbf{x}}[l,k] \triangleq \tilde{\mathbf{H}}_{l,k}\, \mathbf{a}[l,k] \quad \text{with } \tilde{\mathbf{H}}_{l,k} \triangleq \big[\mathbf{H}_{l,k;l,k} \odot \mathbf{D}\big]. \tag{7}$$

Here, the 0/1-valued matrix $\mathbf{D}$ is used to select those channel coefficients that correspond to IPI tolerated at the receiver. If the receiver targets at simple scalar equalization and thus tolerates no IPI, then $\mathbf{D} = \mathbf{I}$. Tolarating all IPI by using more sophisticated matrix equalizers corresponds to $\mathbf{D} = \mathbf{1}$ with $\mathbf{1}$ the all-one matrix. Note that according to (7) ISI, ICI, and noise are always undesired.

Statistical Analysis. We next calculate the statistics of the interference/noise vector $\mathbf{e}[l,k]$. We assume zero-mean, i.i.d. input symbol vectors $\mathbf{a}[l,k]$ with correlation matrix $\mathbf{C_a} \triangleq \mathcal{E}\{\mathbf{a}[l,k]\mathbf{a}[l,k]^H\}$. It then follows from (6) and from the WSSUS and AWGN assumptions that $\mathbf{e}[l,k]$ is 2-D stationary with correlation

$$\mathbf{C_e} \triangleq \mathcal{E}\big\{\mathbf{e}[l,k]\mathbf{e}^H[l,k]\big\} = \mathbf{C_x} - \mathbf{C}_{\mathbf{x},\tilde{\mathbf{x}}} - \mathbf{C}_{\mathbf{x},\tilde{\mathbf{x}}}^H + \mathbf{C}_{\tilde{\mathbf{x}}}, \tag{8}$$

with

$$\mathbf{C_x} = \int_\tau\!\int_\nu \mathcal{C}_{\mathbb{H}}(\tau,\nu)\, \mathbf{A}_{\boldsymbol{\gamma},\mathbf{g}}^*(\tau,\nu)\, \mathbf{C_a}\, \mathbf{A}_{\boldsymbol{\gamma},\mathbf{g}}^T(\tau,\nu)\, d\tau d\nu + \sigma_n^2 \int_t \boldsymbol{\gamma}^*(t)\boldsymbol{\gamma}^T(t)\, dt,$$

$$\mathbf{C}_{\tilde{\mathbf{x}}} = \int_\tau\!\int_\nu C_{\mathbb{H}}(\tau,\nu)\big[\mathbf{A}_{\boldsymbol{\gamma},\mathbf{g}}^*(\tau,\nu) \odot \mathbf{D}\big]\mathbf{C_a}\big[\mathbf{A}_{\boldsymbol{\gamma},\mathbf{g}}^*(\tau,\nu) \odot \mathbf{D}\big]^H d\tau d\nu,$$

$$\mathbf{C}_{\mathbf{x},\tilde{\mathbf{x}}} = \int_\tau\!\int_\nu C_{\mathbb{H}}(\tau,\nu)\, \mathbf{A}_{\boldsymbol{\gamma},\mathbf{g}}^*(\tau,\nu)\, \mathbf{C_a}\big[\mathbf{A}_{\boldsymbol{\gamma},\mathbf{g}}^*(\tau,\nu) \odot \mathbf{D}\big]^H d\tau d\nu.$$

Here, we used a periodized version of the scattering function,

$$\mathcal{C}_{\mathbb{H}}(\tau,\nu) \triangleq \sum_{l=-\infty}^{\infty} \sum_{k=-\infty}^{\infty} C_{\mathbb{H}}(\tau - lT, \nu - kF),$$

and the *matrix cross ambiguity function*

$$\mathbf{A}_{\boldsymbol{\gamma},\mathbf{g}}(\tau,\nu) \triangleq \int_t \boldsymbol{\gamma}(t)\, \mathbf{g}^H(t-\tau) e^{-j2\pi\nu t} dt.$$

Performance Measures. We next present different global performance measures that are based on the error-correlation $\mathbf{C_e}$ and enable us to perform MPMC system optimization.

The first and simplest performance measure is the *average MSE*

$$\varepsilon^2 \triangleq \frac{1}{R}\mathcal{E}\big\{\|\mathbf{e}[l,k]\|_2^2\big\} = \frac{1}{R}\sum_{r=1}^{R}\mathcal{E}\{|e^{(r)}[l,k]|^2\} = \frac{1}{R}\operatorname{tr}\{\mathbf{C_e}\}. \tag{9}$$

This quantity is straightforward to calculate and useful for system performance evaluations. However, it does not describe whether a system is balanced in the sense that the diagonal values of $\mathbf{C_e}$ are approximately equal. If an assessment of the individual MSE components $[\mathbf{C_e}]_{r,r} = \mathcal{E}\{|e^{(r)}[l,k]|^2\}$ is desired, a more appropriate performance measure is the *worst-case MSE*

$$\varepsilon_{\max}^2 \triangleq \max_{r\in\{1,\ldots,R\}} [\mathbf{C_e}]_{r,r}. \tag{10}$$

In contrast to (9), this quantity penalizes unbalanced systems.

From a communication/information theory point of view more meaningful performance measures are mutual information and spectral efficiency. We assume for simplicity that the transmit symbol vectors $\mathbf{a}[l,k]$ and the error vectors $\mathbf{e}[l,k]$ are independent and i.i.d. Gaussian. Then, the mutual information of $\mathbf{a}[l,k]$ and $\mathbf{x}[l,k]$, assuming that $\tilde{\mathbf{H}}_{l,k}$ is known at the receiver, is given by (see [9])

$$I_{l,k} = \log_2 \det\big(\mathbf{I} + \tilde{\mathbf{H}}_{l,k}\mathbf{C_a}\tilde{\mathbf{H}}_{l,k}^H\mathbf{C_e}^{-1}\big).$$

The expectation of $I_{l,k}$ is known as the *ergodic mutual information*, $\bar{I} \triangleq \mathcal{E}_{\mathbb{H}}\{I_{l,k}\}$. It is independent of l, k since the channel is WSSUS. The spectral efficency in (bit/s/Hz) is obtained by normalizing $\bar{I}$ with TF:

$$\zeta \triangleq \frac{1}{TF}\bar{I}. \tag{11}$$

The expectation involved in $\bar{I}$ and ζ is difficult to evaluate. However, since $\log_2 \det(\cdot)$ is convex, an upper bound is obtained according to Jensen's inequality [9],

$$\begin{aligned}\zeta &= \frac{1}{TF}\mathcal{E}_{\mathbb{H}}\{\log_2 \det\big(\mathbf{I} + \tilde{\mathbf{H}}_{l,k}\mathbf{C_a}\tilde{\mathbf{H}}_{l,k}^H\mathbf{C_e}^{-1}\big)\}\\ &\le \frac{1}{TF}\log_2 \det\big(\mathbf{I} + \mathcal{E}_{\mathbb{H}}\{\tilde{\mathbf{H}}_{l,k}\mathbf{C_a}\tilde{\mathbf{H}}_{l,k}^H\}\mathbf{C_e}^{-1}\big) = \zeta_{\max}.\end{aligned}$$

With (7), we obtain

$$\begin{aligned}\mathcal{E}_{\mathbb{H}}\big\{\tilde{\mathbf{H}}_{l,k}\mathbf{C_a}\tilde{\mathbf{H}}_{l,k}^H\big\} &= \mathcal{E}_{\mathbb{H}}\big\{\mathcal{E}_{\mathbf{a}}\big\{\tilde{\mathbf{H}}_{l,k}\mathbf{a}[l,k]\,\mathbf{a}^H[l,k]\tilde{\mathbf{H}}_{l,k}^H\big\}\big\}\\ &= \mathcal{E}\big\{\tilde{\mathbf{x}}[l,k]\,\tilde{\mathbf{x}}^H[l,k]\big\} = \mathbf{C}_{\tilde{\mathbf{x}}}.\end{aligned}$$

Thus, the upper bound $\zeta_{\max}$ on the spectral efficiency equals

$$\zeta_{\max} = \frac{1}{TF}\log_2 \det\big(\mathbf{I} + \mathbf{C}_{\tilde{\mathbf{x}}}\,\mathbf{C_e}^{-1}\big). \tag{12}$$

In our simulations we observed that typically $\zeta_{\max}$ is close to ζ. Although slightly more difficult to compute than the MSE measures ε^2 and $\varepsilon_{\max}^2$, $\zeta_{\max}$ has the advantage of being a more direct indicator of the overall system performance.

4. SYSTEM OPTIMIZATION

Based on the performance measures of the previous section, we next propose algorithms and guidelines for MPMC system optimization for prescribed channels with scattering function $C_{\mathbb{H}}(\tau,\nu)$ and noise variance σ_n^2. We propose a successive separate optimization of transmit/receive pulses, symbol power allocation, and TF lattice parameters since joint optimization is difficult.

Pulse Optimization. We first attempt to choose a receive pulse $\boldsymbol{\gamma}(t)$ that is biorthogonal to a fixed, prescribed transmit pulse $\mathbf{g}(t)$ and that minimizes the average MSE $\varepsilon^2 = \frac{1}{R}\mathrm{tr}\{\mathbf{C_e}\}$ (all system parameters other than $\boldsymbol{\gamma}(t)$ are considered fixed). This is possible since for $TF > R$, the receive pulse $\boldsymbol{\gamma}(t)$ is not uniquely determined by the biorthogonality condition (4). In particular, any biorthogonal receive pulse vector can be written as

$$\boldsymbol{\gamma}(t) = \boldsymbol{\gamma}_0(t) + \mathbf{V}\,\mathbf{u}(t). \tag{13}$$

Here, $\boldsymbol{\gamma}_0(t)$ is the *canonical biorthogonal pulse* (cf. [1]), $\mathbf{u}(t) = [u^{(1)}(t) \ldots u^{(L_u)}(t)]^T$ is a length-L_u vector[2] such that $\mathrm{span}\{u^{(i)}(t)\} = \mathcal{S}^{\perp}$ where $\mathcal{S} = \mathrm{span}\{g_{l,k}^{(r)}(t)\}$, and $\mathbf{V} = [\mathbf{v}^{(1)} \ldots \mathbf{v}^{(R)}]^T$ is an arbitrary $R \times L_u$ coefficient matrix.

By virtue of (13), constrained minimization of ε^2 (cf. (9)) with respect to $\boldsymbol{\gamma}(t)$ is equivalent to unconstrained minimization with respect to $\mathbf{V}$. It can be shown that $[\mathbf{C_e}]_{r,r}$, $r = 1, \ldots R$, is a quadratic functional of $\mathbf{v}^{(r)}$ and does not depend on $\mathbf{v}^{(r')}$, $r' \neq r$; $\mathrm{tr}\{\mathbf{C_e}\}$ can thus be minimized by separately minimizing $[\mathbf{C_e}]_{r,r}$ with respect to $\mathbf{v}^{(r)}$. Assuming diagonal $\mathbf{C_a}$, this amounts to solving the R linear equations $\big(\mathbf{W_x} - \mathbf{W}_{\tilde{\mathbf{x}}}^{(r)}\big)\mathbf{v}^{(r)} = \mathbf{y}_{\mathbf{x}}^{(r)} - \mathbf{y}_{\tilde{\mathbf{x}}}^{(r)}$. Here,

$$\mathbf{W_x} = \int_{\tau}\!\int_{\nu} \mathcal{C}_{\mathbb{H}}(\tau,\nu)\,\mathbf{A}^*_{\mathbf{u},\mathbf{g}}(\tau,\nu)\mathbf{C_a}\,\mathbf{A}^T_{\mathbf{u},\mathbf{g}}(\tau,\nu)\,d\tau\, d\nu + \sigma_n^2 \int_t \mathbf{u}^*(t)\mathbf{u}^T(t)\,dt,$$

$$\mathbf{W}_{\tilde{\mathbf{x}}}^{(r)} = \int_{\tau}\!\int_{\nu} C_{\mathbb{H}}(\tau,\nu)\,\mathbf{A}^*_{\mathbf{u},\mathbf{g}}(\tau,\nu)\,\mathbf{D}^{(r)}\mathbf{C_a}\,\mathbf{A}^T_{\mathbf{u},\mathbf{g}}(\tau,\nu)\,d\tau\, d\nu,$$

$$\mathbf{y}_{\mathbf{x}}^{(r)} = \int_{\tau}\!\int_{\nu} \mathcal{C}_{\mathbb{H}}(\tau,\nu)\mathbf{A}^*_{\mathbf{u},\mathbf{g}}(\tau,\nu)\mathbf{C_a}\,\mathbf{A}^T_{\gamma_0^{(r)},\mathbf{g}}(\tau,\nu)\,d\tau\, d\nu + \sigma_n^2 \int_t \mathbf{u}^*(t)\gamma_0^{(r)}(t)\,dt,$$

$$\mathbf{y}_{\tilde{\mathbf{x}}}^{(r)} = \int_{\tau}\!\int_{\nu} C_{\mathbb{H}}(\tau,\nu)\,\mathbf{A}^*_{\mathbf{u},\mathbf{g}}(\tau,\nu)\,\mathbf{D}^{(r)}\mathbf{C_a}\,\mathbf{A}^T_{\gamma_0^{(r)},\mathbf{g}}(\tau,\nu)\,d\tau\, d\nu.$$

with $\mathbf{D}^{(r)}$ the $R \times R$ diagonal matrix with entries $\big[\mathbf{D}^{(r)}\big]_{i,i} = [\mathbf{D}]_{r,i}$. This yields $\mathbf{v}_{\mathrm{opt}}^{(r)} = \big(\mathbf{W_x} - \mathbf{W}_{\tilde{\mathbf{x}}}^{(r)}\big)^{-1}\big(\mathbf{y}_{\mathbf{x}}^{(r)} - \mathbf{y}_{\tilde{\mathbf{x}}}^{(r)}\big)$. Hence, the optimum biorthogonal receive pulse is given by

$$\boldsymbol{\gamma}_{\mathrm{opt}}(t) = \boldsymbol{\gamma}_0(t) + \mathbf{V}_{\mathrm{opt}}\,\mathbf{u}(t)$$

where $\mathbf{V}_{\mathrm{opt}} = \big[\mathbf{v}_{\mathrm{opt}}^{(1)} \ldots \mathbf{v}_{\mathrm{opt}}^{(R)}\big]^T$. This pulse design extends the methods for single-pulse systems in [2].

Power Allocation. We next consider maximization of $\zeta_{\max}$ by optimizing the power allocation $P_r \triangleq \mathcal{E}\{a^{(r)}[l,k]\}$. We assume uncorrelated transmit symbols $a^{(r)}[l,k]$ such that $\mathbf{C_a} = \mathrm{diag}\{P_1, \ldots, P_R\}$. Furthermore, $\mathrm{tr}\{\mathbf{C_a}\} = \sum_{r=1}^{R} P_r$ (which is proportional to the mean transmit power) is assumed fixed. At first glance, it appears that this optimization problem can be solved via a water-filling algorithm (cf. [9]). However, this is not the case since the statistics of $\mathbf{e}[l,k]$ depend on $\mathbf{C_a}$ (cf. (8)). Since we did not succeed in solving the optimum power allocation problem analytically, we propose a numerical optimization based on the MATLAB Optimization Toolbox.

Lattice Parameters. We determine the lattice parameters T, F indirectly by choosing the *shape factor* $\frac{T}{F}$ and the *redundancy* $\frac{TF}{R}$. While a numerical optimization of the shape factor $\frac{T}{F}$ could be performed, symmetry arguments suggest the choice (cf. [3, 6] for the case $R = 1$)

$$\frac{T}{F} = \frac{\tau_{\max}}{\nu_{\max}}, \tag{14}$$

[2]While L_u in general is infinite, it is finite for practical discrete implementations.

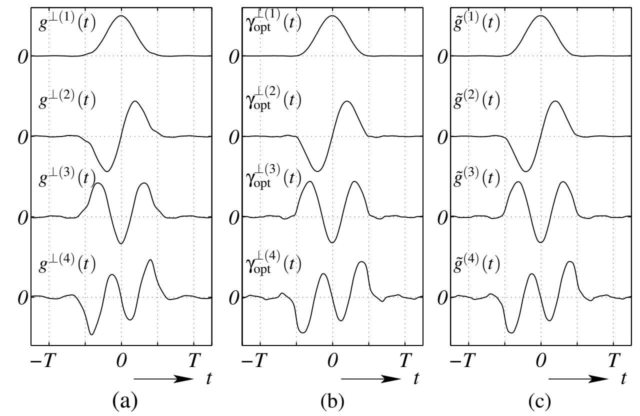

Figure 2: *MPMC pulses: (a) orthogonalized pulse $\mathbf{g}^{\perp}(t)$, (b) optimum biorthogonal pulse $\boldsymbol{\gamma}_{opt}^{\perp}(t)$, (c) pulse $\tilde{\mathbf{g}}(t)$ obtained via joint iterative optimization.*

where $\tau_{\max}$ and $\nu_{\max}$ denote the channel's maximum delay and maximum Doppler frequency. The choice of the redundancy $\frac{TF}{R}$ is guided by the conflicting goals of large symbol rate (obtained with small $\frac{TF}{R}$) and weak interference (obtained with large $\frac{TF}{R}$, due to reduced overlap of adjacent pulses). Since both of these criteria are captured by the spectral efficiency bound $\zeta_{\max}$ in (12), we propose to numerically optimize $\frac{TF}{R}$ (with all other system parameters fixed) such that $\zeta_{\max}$ is maximized.

Joint Iterative Optimization. To combine the gains achieved by the separate optimization of pulse shapes, power allocation, and lattice parameters, the individual optimizations can be combined in an iterative fashion. Within each iteration loop, pulse optimization, optimum power allocation, and lattice optimization can be performed successively. In our simulations, we achieved the best results by starting with an orthogonalized pulse with fixed redundancy, choosing the shape factor according to (14), and then performing the following steps within each iteration loop: 1) calculation of optimum biorthogonal pulse, 2) orthogonalization of the resulting pulse, and 3) numerical optimization of the power allocation. This procedure typically converged to a stable solution after a few iterations.

5. SIMULATION RESULTS

Our simulations illustrate the optimization gains for MPMC systems with $R = 4$ and $\mathbf{D} = \mathbf{1}$ (i.e. matrix equalization at the receiver). The initial transmit pulse $\mathbf{g}(t)$ consists of the first four Hermite functions. We assume a channel with a scattering function that equals the indicator function of $[-\tau_{\max}, \tau_{\max}] \times [-\nu_{\max}, \nu_{\max}]$. The shape factor was chosen according to (14).

Experiment 1. We first consider a fixed redundancy $TF/R = 1.15$, a channel with spread factor $4\tau_{\max}\nu_{\max} = 0.01$, and SNR $= 30$ dB. In this situation, an absolute upper bound for $\zeta_{\max}$ (assuming only noise and no interference) is 8.67 bit/s/Hz.

Let us first investigate pulse optimization for uniform power allocation ($\mathbf{C_a} = \mathbf{I}$). From $\mathbf{g}(t)$, the canonical biorthogonal receive pulse $\boldsymbol{\gamma}(t)$ and the orthogonalized transmit/receive pulse $\mathbf{g}^{\perp}(t)$ (cf. Fig. 2(a)) can be calculated according to [1], leading to a maximum spectral efficiency of $\zeta_{\max} = 7.35$ bit/s/Hz for $\{\mathbf{g}(t), \boldsymbol{\gamma}(t)\}$ and $\zeta_{\max} = 7.85$ bit/s/Hz for $\{\mathbf{g}^{\perp}(t), \mathbf{g}^{\perp}(t)\}$. Using the optimized receive pulses $\boldsymbol{\gamma}_{\mathrm{opt}}(t)$ and $\boldsymbol{\gamma}_{\mathrm{opt}}^{\perp}(t)$, that are biorthogonal to $\mathbf{g}(t)$ and

transmit pulse	receive pulse	ζ_{max} [bit/s/Hz]	
		$\mathbf{C_a} = \mathbf{I}$	$\mathbf{C}_{\mathbf{a},\mathrm{opt}}$
$\mathbf{g}(t)$	$\boldsymbol{\gamma}(t)$	7.35	7.91
$\mathbf{g}^{\perp}(t)$	$\mathbf{g}^{\perp}(t)$	7.85	8.02
$\mathbf{g}(t)$	$\boldsymbol{\gamma}_{\mathrm{opt}}(t)$	7.95	8.10
$\mathbf{g}^{\perp}(t)$	$\boldsymbol{\gamma}^{\perp}_{\mathrm{opt}}(t)$	8.11	8.16
$\tilde{\mathbf{g}}(t)$	$\tilde{\mathbf{g}}(t)$	-	8.30

Table 1: *Spectral efficiencies of various MPMC systems.*

$\mathbf{g}^{\perp}(t)$ respectively, the spectral efficiency can be improved to $\zeta_{max} = 7.95$ bit/s/Hz and $\zeta_{max} = 8.11$ bit/s/Hz (cf. Fig. 2(b) and Table 1).

We next improve the foregoing MPMC systems by using the optimized power allocation $\mathbf{C}_{\mathbf{a},\mathrm{opt}}$ (while leaving all other system parameters fixed). The resulting spectral efficiencies ζ_{max} are shown in the right-most column of Table 1, verifying further noticeable performance gains. E.g., optimized power allocation improves the canonical biorthogonal MPMC system $\{\mathbf{g}(t), \boldsymbol{\gamma}(t)\}$ from $\zeta_{max} = 7.35$ bits/s/Hz (with $\mathbf{C_a} = \mathbf{I}$) to $\zeta_{max} = 7.91$ bits/s/Hz (with $\mathbf{C}_{\mathbf{a},\mathrm{opt}} = \mathrm{diag}\{1.23, 1.23, 1.43, 0.11\}$).

We next perform joint iterative optimization of pulse shapes and power allocation, starting with the transmit pulse $\mathbf{g}^{\perp}(t)$ (consisting of the $R = 4$ Hermite functions) and with uniform power allocation. With only three iteration loops we obtained an optimized (orthogonal) MPMC system with pulses $\tilde{\mathbf{g}}(t)$ shown in Fig. 2(c) and power allocation $\mathbf{C}_{\mathbf{a},\mathrm{opt}} = \mathrm{diag}\{1.19, 1.18, 1.13, 0.50\}$. The spectral efficiency bound for this system equals $\zeta_{max} = 8.30$ bit/s/Hz. Compared to the conventional system design (canonical biorthogonal pulse, uniform power allocation), this is an improvement of 0.95 bit/s/Hz. The gap to the interference free spectral efficiency of 8.67 bit/s/Hz is only 0.37 bit/s/Hz.

Experiment 2. We next investigate the dependence of ζ_{max} on the TF lattice parameters for MPMC systems with $R = 4$ and $\mathbf{C_a} = \mathbf{I}$. We redesigned the system $\{\mathbf{g}^{\perp}(t), \boldsymbol{\gamma}^{\perp,\mathrm{opt}}(t)\}$ for various redundancies $\frac{TF}{R} \in [1.025, 1.3]$, starting with Hermite initial pulses. The maximum spectral efficiency ζ_{max} obtained for the various redundancies is depicted in Fig. 3(a) for SNRs of 20 and 30 dB and various channel spread factors $4\tau_{max}\nu_{max} \in \{0, 0.0025, 0.01\}$.

For comparison, we optimized a conventional single-pulse MC system ($R = 1$) for the same redundancies, starting from a Gaussian transmit pulse[3] (i.e., the first Hermite function). The result is depicted in Fig. 3(b).

It is seen that the MPMC system consistently outperforms the single-pulse system, with a gain of more than 1 bit/s/Hz in the interference-limited case (SNR=30 dB and $4\tau_{max}\nu_{max} = 0.01$). It is further seen that the MPMC system is more robust against channel dispersion in the sense that for a certain choice of TF/R, the spectral efficiency of the MPMC system depends much less on the channel spread than that of the single-pulse system. Finally, for given channel parameters, both systems feature an optimum redundancy TF/R for which ζ_{max} is maximum. This optimum redundancy decreases with decreasing SNR (noise limited case) and increases with increasing channel spread (interference limited case). Note however, that the optimum redundancy of the MPMC system depends much less on the channel parameters.

[3]MC systems with orthogonalized Gaussian pulses have been proposed in [6] and can equivalently be obtained by the so-called IOTA approach [10].

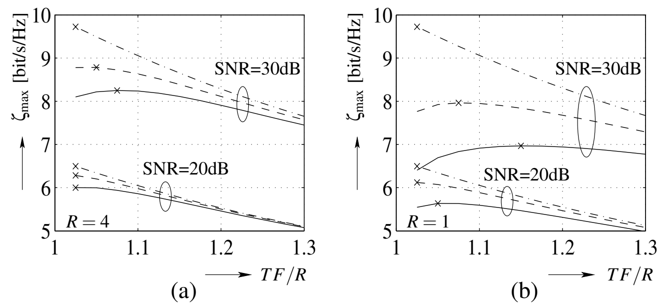

Figure 3: *Spectral efficiency bound ζ_{max} versus TF/R for (a) optimized MPMC system and (b) optimized single-pulse MC system for different SNRs and channel spread factors $4\tau_{max}\nu_{max}$ equal to 0 (dash-dotted), 0.0025 (dashed), 0.01 (solid).*

6. CONCLUSIONS

We considered a recently introduced communication scheme termed multipulse multicarrier (MPMC) modulation and performed an interference analysis of MPMC transmissions over random time-varying channels. Based on this analysis, we defined various system performance measures and developed algorithms and guidelines for optimizing pulse shapes, power allocation, and time-frequency lattice parameters of MPMC systems. Numerical simulations showed significant optimization gains as well as the superiority of MPMC systems over traditional single-pulse multicarrier systems.

REFERENCES

[1] M. M. Hartmann, G. Matz, and D. Schafhuber, “Theory and design of multipulse multicarrier systems for wireless communications,” in *Proc. 37th Asilomar Conf. Signals, Systems, Computers*, (Pacific Grove, CA), Nov. 2003.

[2] D. Schafhuber, G. Matz, and F. Hlawatsch, “Pulse-shaping OFDM/BFDM systems for time-varying channels: ISI/ICI analysis, optimal pulse design, and efficient implementation,” in *Proc. IEEE PIMRC-02*, (Lisbon, Portugal), pp. 1012–1016, Sept. 2002.

[3] W. Kozek and A. F. Molisch, “Nonorthogonal pulseshapes for multicarrier communications in doubly dispersive channels,” *IEEE J. Sel. Areas Comm.*, vol. 16, pp. 1579–1589, Oct. 1998.

[4] S. Hara and R. Prasad, “Overview of multicarrier CDMA,” *IEEE Comm. Mag.*, vol. 35, pp. 126–133, Dec. 1997.

[5] H. Bölcskei, P. Duhamel, and R. Hleiss, “Design of pulse shaping OFDM/OQAM systems for high data-rate transmission over wireless channels,” in *Proc. IEEE ICC-99*, (Vancouver, Canada), pp. 559–564, June 1999.

[6] T. Strohmer and S. Beaver, “Optimal OFDM design for time-frequency dispersive channels,” *IEEE Trans. Comm.*, vol. 51, pp. 1111–1122, July 2003.

[7] P. A. Bello, “Characterization of randomly time-variant linear channels,” *IEEE Trans. Comm. Syst.*, vol. 11, pp. 360–393, 1963.

[8] J. G. Proakis, *Digital Communications*. New York: McGraw-Hill, 3rd ed., 1995.

[9] T. M. Cover and J. A. Thomas, *Elements of Information Theory*. New York: Wiley, 1991.

[10] B. LeFloch, M. Alard, and C. Berrou, “Coded orthogonal frequency division multiplex,” *Proc. IEEE*, vol. 83, pp. 982–996, June 1995.